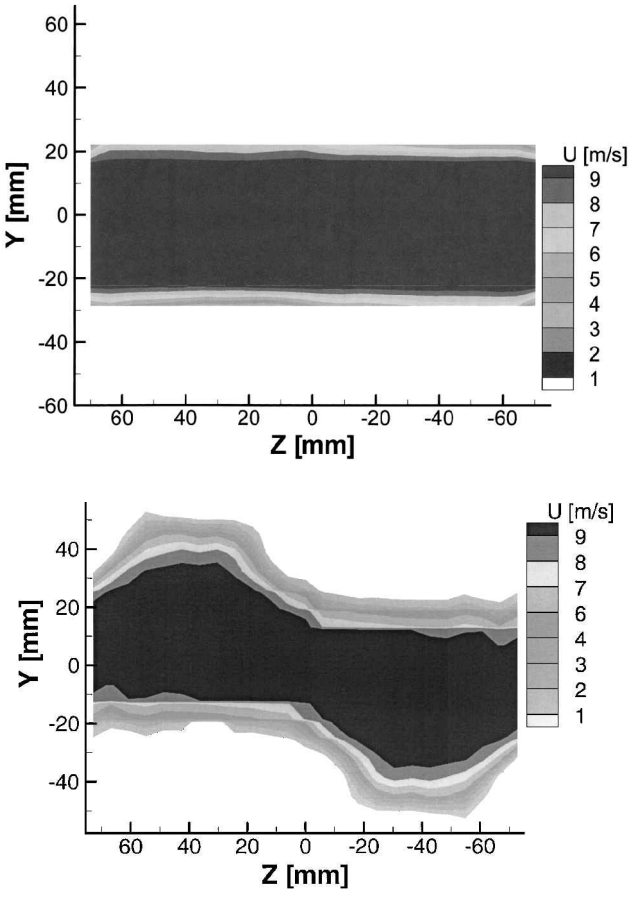

Fig. 4 Mean velocity contours of flow at $x = 25.4$ mm, X and R actuator excitation, $\langle c\mu \rangle = 4\%$: a) baseline flow and b) controlled flow.

identification of the angle generated between the jet principle axis and the Z axis, using the flow visualization pictures (not shown) and taking into account the smoke density, using the 8-bit grayscale resolution. These calculations indicate that the jet was rotated by 13 ± 4 deg at $x/d_h = 0.33$, with respect to the baseline condition.

To verify that the measured data are indicative of jet rotation, and not only modification of the jet velocity distribution at the exit plane, additional flow visualization pictures were acquired at distances of 76.2 and 127.0 mm from the jet exit plane (not shown). The rotational momentum of the free jet should be conserved, so that the observed rotation angle is expected to increase as the observation plane is moved in the streamwise direction. Indeed, the flow visualization images that were acquired farther downstream validate this trend (not shown). The controlled jet data exhibits the same features as the measurements made at $x = 25.4$ mm, but the rotation angle, evaluated using identification of the major axis, is 30 ± 4 deg at $x = 127.0$ mm ($x/d_h = 1.67$), a significant increase with respect to the rotation angle measured at $x = 25.4$ mm. The use of two different excitation frequencies, disregarding the relative phase between the two pairs of actuators is not optimal.

Conclusions

The results clearly demonstrate that a rectangular jet can be rotated using properly placed and directed actuators. The method demonstrated in this Note should allow jet rotation without moving parts, with short-duration transients and in a controlled and gradual manner.

Acknowledgments

The experiment was performed while the first and last authors were visiting ICASE, NASA Langley Research Center. The help and support provided by Richard White and Luther Jenkins are greatly appreciated. Many helpful comments were provided by S. P. Wilkinson, who reviewed the manuscript.

References

[1]Pack, L. G., and Seifert, A., "Periodic Excitation for Jet Vectoring and Enhanced Spreading," *Journal of Aircraft*, June 2001; also AIAA Paper 99-0672, Jan. 1999.

[2]Pack, L. G., and Seifert, A., "Multiple Mode Actuation of a Turbulent Jet," AIAA Paper 01-0735, Jan. 2001.

[3]Seifert, A., Bachar, T., Koss, D., Shepshelovits, M., and Wygnanski, I., "Oscillatory Blowing, a Tool to Delay Boundary Layer Separation," *AIAA Journal*, Vol. 31, No. 11, 1993, pp. 2052–2060.

[4]Seifert, A., Darabi, A., and Wygnanski, I., "Delay of Airfoil Stall by Periodic Excitation," *Journal of Aircraft*, Vol. 33, No. 4, 1996, pp. 691–699.

[5]Smith, B. L., and Glezer, A., "Vectoring and Small-Scale Motions Effected in Free Shear Flows Using Synthetic Jet Actuators," AIAA Paper 97-0213, Jan. 1997.

Side Force on a Rough-Surface Ogive Cylinder: Effects of Freestream Turbulence

K. B. Lua* and S. C. Luo†
National University of Singapore, Singapore 119260, Republic of Singapore
and
E. K. R. Goh‡
Defence Science Organization National Laboratories, Singapore 118230, Republic of Singapore

Nomenclature

A	=	axial distance from model nose tip
b	=	grid bar diameter
C_p	=	pressure coefficient, $(p - p_\infty)/(0.5\rho U_\infty^2)$
C_y	=	side force coefficient, $F_y/(0.5\rho U_\infty^2 S)$
$C_y(A)$	=	local side force coefficient, local side force/$(0.5\rho U_\infty^2 D \sin^2 \alpha)$
$\lvert C_y \rvert$	=	absolute value of the side force coefficient
$\lvert \overline{C_y} \rvert$	=	mean of the absolute value of all of the side force coefficients in the $0 \le \phi < 360$ deg range
D	=	cylinder diameter
d_{particle}	=	average diameter of aluminum oxide particles
F_y	=	side force
I	=	turbulence intensity
I_x	=	longitudinal turbulence intensity in freestream direction, σ_x/U_∞
L	=	turbulence length scale
L_x	=	longitudinal turbulence length scale in the freestream direction
M	=	mesh opening length
P	=	pressure on model surface

Received 24 February 2002; revision received 30 April 2002; accepted for publication 1 May 2002. Copyright © 2002 by the authors. Published by the American Institute of Aeronautics and Astronautics, Inc., with permission. Copies of this paper may be made for personal or internal use, on condition that the copier pay the $10.00 per-copy fee to the Copyright Clearance Center, Inc., 222 Rosewood Drive, Danvers, MA 01923; include the code 0021-8669/03 $10.00 in correspondence with the CCC.

*Research Fellow, Department of Mechanical Engineering, 10 Kent Ridge Crescent.

†Associate Professor, Department of Mechanical Engineering, 10 Kent Ridge Crescent.

‡Senior Member of the Technical Staff, Aeronautic Systems Program, 20 Science Park Drive.

P_∞ = freestream static pressure
Re_D = Reynolds number, $U_\infty D/\nu$
S = model base area, $\pi D^2/4$
U_∞ = time average freestream velocity
α = angle of attack
θ = azimuth angle around circular cross section measured from the most leeward position
ν = kinematic viscosity of fluid
ρ = density of fluid
ϕ = roll angle

Introduction

In a related paper,[1] the effects of surface roughness with $d_{\text{particle}}/D = 0.0093$ on (smooth) flow past a 50-deg inclined ogive cylinder was studied. The surface roughness was found to cause a laminar to turbulent transition in the boundary layer(s) of the cylinder. To continue the study, the present investigation looks into the effects of the intensity I and length scale L of turbulence in the freestream. To study the effects of the two separately, the turbulence intensity and length scale of the freestream were varied one at a time. To achieve that, turbulence was created by placing different turbulence generating grids (one at a time), at different distances upstream of the model.

Experimental Apparatus and Techniques

The wind tunnel used, the rough surface model, and the way to measure side force and surface pressure distribution are all identical to those reported by Luo et al.[1,2] Thus, for brevity, they will not be repeated here. Also, as in Ref. 1, the angle of attack α was fixed at 50 deg and the Reynolds number Re_D at 3.5×10^4.

To generate freestream turbulence, five sets of biplanar square-mesh grids were used in the present investigation. The five similar biplanar square-mesh grids were made from round bars with diameters 3, 6, 9, 12, and 15 mm. The grid opening M to bar diameter b ratio M/b was fixed at 5 for all of the grids. The purpose of having several grids was to vary the length scale of the turbulence because the length scale would be proportional to the size of the grid opening.

Results and Discussion

The study of the effects of freestream turbulence consists of two parts. In the first part, the length scale L_x is kept constant at $L_x/D = 0.354, 0.428$, or 0.575, whereas the turbulence intensity I_x is varied from 0.72 to 3.91%. In the second part, the intensity level is kept constant at either 1.92, 2.91, or 3.91%, whereas the turbulence length scale is varied from $L_x/D = 0.252$ to 0.569.

The results, which correspond to the dimensionless turbulence length scale L_x/D fixed at 0.428 and the I_x varied from 0.72 to 3.91% are shown in Fig. 1, together with the results with no grid installed. It can be seen that in a turbulent flow, the magnitude of the fluctuations in the side force distribution are smaller as the flow has become less sensitive to small geometrical imperfections of the model. Generally speaking, the freestream turbulence has further reduced the magnitude of side force. For example, the maximum side force coefficient has been reduced from $C_y = +3.2$ and -3.42 (no grid) to $C_y = +2.59$ and -2.36 when $I_x = 0.72\%$. For all of the length scales tested, a further increase in I_x appears to result in a further (but slight) reduction in the side force magnitude, although no clear trend can be detected. To provide a more objective and quantitative comparison for the four cases shown in Fig. 1, we compute the standard deviation (SDEV) and the mean of the magnitude (i.e., the negative sign is ignored for forces that point in the negative direction) of all of the side force data in the $0 \le \phi < 360$ deg range by using the formulae

$$\text{SDEV} = \sqrt{\left[N \sum_i^N C_{y_i}^2 - \left(\sum_i^N C_{y_i} \right)^2 \right] \Big/ N^2}$$

and

$$|\overline{C_y}| = \sum_{i=1}^{N} |C_{y_i}| \Big/ N$$

respectively. In the preceding equations, N is the total number of the C_{y_i} data. The magnitudes of SDEV and $|\overline{C_y}|$ for $I_x = 0.72, 2.22,$

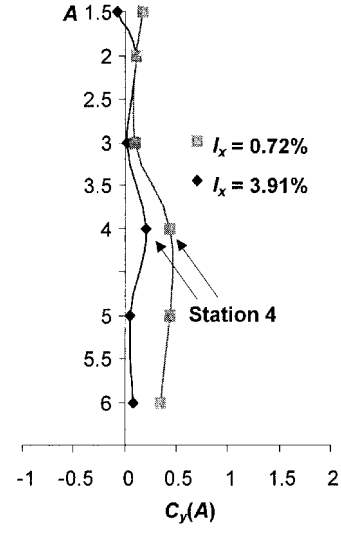

Fig. 2a Local side force distributions for the rough surface models at $\phi = 208.8$ deg with $I_x = 0.72$ and 3.91% and $L_x/D = 0.428$.

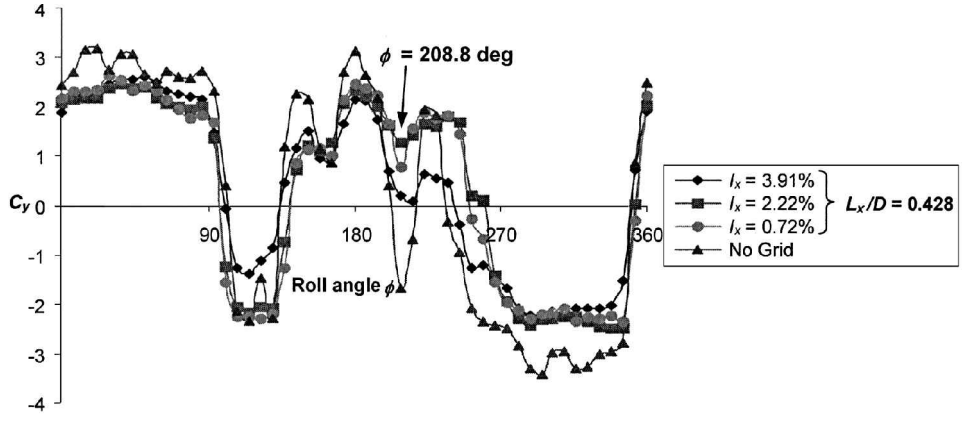

Fig. 1 Effects of varying turbulence intensity I_x on the rough surface model's C_y vs ϕ plot at $L_x/D = 0.428$.

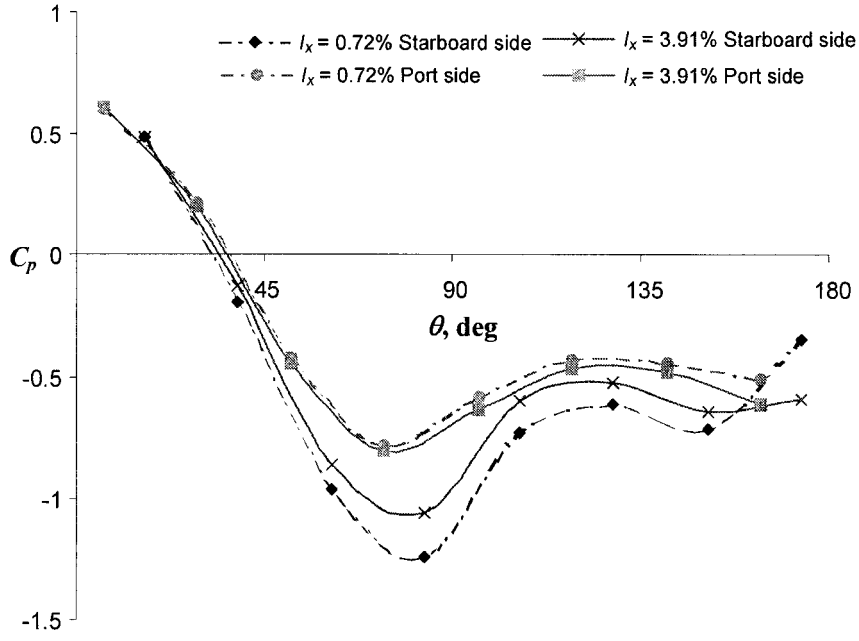

Fig. 2b Pressure distributions at station 4 for both conditions.

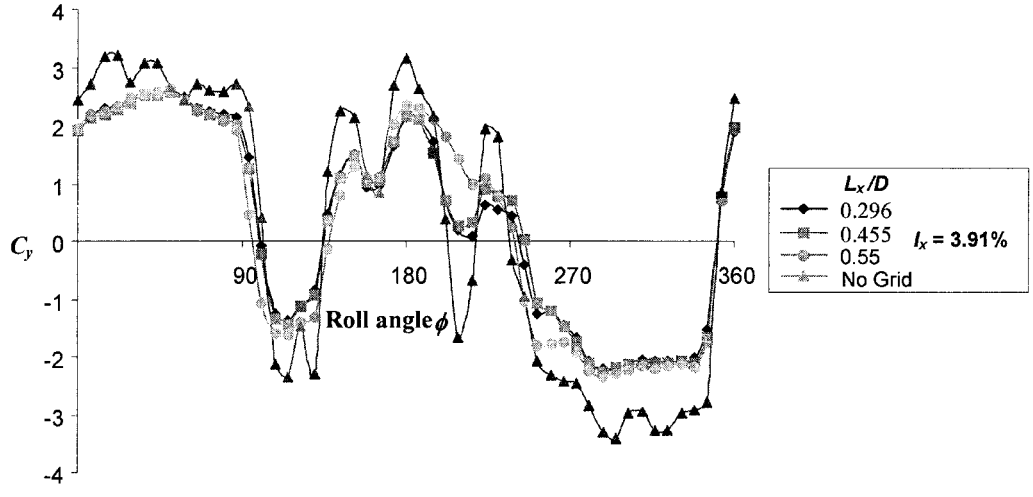

Fig. 3 Effects of varying the turbulence length scale L_x on the C_y vs ϕ plot at turbulence intensity $I_x = 3.91\%$.

Table 1 Effects of varying turbulence intensity I_x at $L_x/D = 0.428$

I_x, %	$\lvert\overline{C_y}\rvert$	SDEV
0.72	1.881	1.933
2.22	1.825	1.893
3.91	1.582	1.704

and 3.91% are shown in Table 1. The results clearly demonstrate that an increase in freestream turbulence reduces both the SDEV and $|\overline{C_y}|$. However, note that the side force reduction achieved in the present work is less significant than that observed by Howard et al.[3] In the experiment of Howard et al.,[3] the maximum side force reduces from −4.2 to −1.0 as the turbulence intensity changes from $I_x = 0.23$ (no grid) to 3.8% [grid installed, turbulence dissipation length scale equal to 43.2 mm (1.7 in.)].

Figure 2 compares the pressure distribution measured at station 4 (see Fig. 2a) and $\phi = 208.8$ deg, between the lowest and highest turbulence intensity tested at $L_x/D = 0.428$. The pressure distributions show that additional turbulence intensity does not significantly alter the structure of the flow (the general shape of the pressure distribution remains unchanged), but reduces the difference in the wake pressure between the two sides, leading to the reduction in side force that had been noted and reported earlier. The difference in turbulence intensity between $I_x = 0.72$ and 3.91% also shows no obvious effect on the flow separation positions on both sides of the cylinder. This suggests that changes in the turbulence intensity (at least in the present range) do not alter the main features of the flow structure.

Figure 3 shows the results of changing L_x at fixed turbulence intensity I_x of 3.91%. In contrast to the case of varying I_x at constant L_x shown in Fig. 1, a smaller turbulence length scale is found to be more effective in reducing the side force. Probably due to the relatively small range in L_x/D used (0.296–0.55), for the majority of the roll angle range, the three sets of turbulent flow data (at different L_x/D) are very close to each other. The only exception appears to be the narrow ϕ range of 187.2–230.4 deg, where the side force associated with the largest of the three length scales ($L_x/D = 0.55$) appears to be clearly larger in magnitude than those of the other two length scales. The SDEV and $|\overline{C_y}|$ for $L_x/D = 0.296$, 0.455, and 0.55 (shown in Table 2) show a similar trend. The magnitudes of SDEV and $|\bar{C}_y|$ decrease when L_x/D decreases. (Note that there is one exception, in that, when L_x/D increases from 0.296 to

Table 2 Effects of varying the turbulence length scale L_x/D at $I_x = 3.91\%$

L_x/D	$\lvert\overline{C_y}\rvert$	SDEV
0.296	1.582	1.704
0.455	1.595	1.703
0.55	1.757	1.844

0.455, SDEV actually decreases from 1.704 to 1.703, which goes against the overall trend. However, this difference is thought to be negligible.)

Conclusions

The effects of freestream turbulence on the side force acting on an ogive cylinder coated with aluminium alloy particles at high angle of attack have been studied experimentally over a range of turbulence intensities and length scales. In a turbulent flow, and within the range of parameters investigated, side force and surface pressure measurements clearly show that, at $\alpha = 50$ deg, an increase in the turbulence intensity (at a constant length scale) causes the side force to decrease. On the other hand, one needs to reduce the turbulence length scale (at a constant turbulence intensity), to achieve a reduction in side force. In the present case, the smallest $L_x/D(0.296)$ appears to have the greatest influence in reducing the side force acting on the ogive cylinder.

References

[1]Luo, S. C., Lua, K. B., and Goh, E. K. R., "Side Force on an Ogive Cylinder: Effects of Surface Roughness," *Journal of Aircraft*, Vol. 39, No. 4, 2002, pp. 716–718.

[2]Luo, S. C., Lua, K. B., and Lim, T. T., "Side Force on an Ogive Cylinder: Effects of Freestream Turbulence," *AIAA Journal*, Vol. 39, No. 12, 2001, pp. 2409–2411.

[3]Howard, R. M., Rabang, M. P., and Roane, D. P., Jr., "Aerodynamic Effects of a Turbulent Flowfield on a Vertically Launched Missile," *Journal of Spacecraft*, Vol. 26, No. 6, 1989, pp. 445–451.